Heteromeric association creates a P2Y-like adenosine receptor

Kazuaki Yoshioka*†, Osamu Saitoh*, and Hiroyasu Nakata*‡

*Department of Molecular and Cellular Neurobiology, Tokyo Metropolitan Institute for Neuroscience, Fuchu, Tokyo 183-8526, Japan; and †Japan Science and Technology Corporation, Kawaguchi, Saitama 332-0012, Japan

Edited by John W. Daly, National Institutes of Health, Bethesda, MD, and approved April 11, 2001 (received for review December 12, 2000)

Adenosine and its endogenous precursor ATP are main components of the purinergic system that modulates cellular and tissue functions via specific adenosine and ATP receptors (P1 and P2 receptors), respectively. Although adenosine inhibits excitability and ATP functions as an excitatory transmitter in the central nervous system, little is known about the ability of P1 and P2 receptors to form new functional structures such as a heteromer to control the complex purinergic cascade. Here we have shown that $G_{i/o}$ protein-coupled A_1 adenosine receptor (A_1R) and G_q protein-coupled $P2Y_1$ receptor ($P2Y_1R$) coimmunoprecipitate in cotransfected HEK293T cells, suggesting the oligomeric association between distinct G protein-coupled P1 and P2 receptors. A_1R and $P2Y_2$ receptor, but not A_1R and dopamine D_2 receptor, also were found to coimmunoprecipitate in cotransfected cells. A_1R agonist and antagonist binding to cell membranes were reduced by coexpression of A_1R and $P2Y_1R$, whereas a potent $P2Y_1R$ agonist adenosine 5′-*O*-(2-thiotriphosphate) (ADPβS) revealed a significant potency to A_1R binding only in the cotransfected cell membranes. Moreover, the A_1R/$P2Y_1R$ coexpressed cells showed an ADPβS-dependent reduction of forskolin-evoked cAMP accumulation that was sensitive to pertussis toxin and A_1R antagonist, indicating that ADPβS binds A_1R and inhibits adenylyl cyclase activity via $G_{i/o}$ proteins. Also, a high degree of A_1R and $P2Y_1R$ colocalization was demonstrated in cotransfected cells by double immunofluorescence experiments with confocal laser microscopy. These results suggest that oligomeric association of A_1R with $P2Y_1R$ generates A_1R with $P2Y_1R$-like agonistic pharmacology and provides a molecular mechanism for an increased diversity of purine signaling.

Adenosine and ATP are two major neurotransmitter and neuromodulating systems that share a number of structural and functional characteristics. These purinergic systems modulate many physiological processes, including smooth muscle contraction, immune response, platelet aggregation, pain, cardiac function, cardioprotection, and neurotransmission (1). Pharmacological and molecular cloning studies have identified two purinergic receptor families, named adenosine receptor or P1 receptor and ATP receptor or P2 receptor. P1 receptors have been further subdivided into A_1R, $A_{2A}R$, $A_{2B}R$, and A_3R, all of which are G protein-coupled receptors (GPCRs). A_1 and A_3 adenosine receptors are coupled to the inhibition of adenylyl cyclase via $G_{i/o}$ proteins. A_{2A} and A_{2B} adenosine receptors are coupled to stimulation of adenylyl cyclase via G_s proteins. P2 receptors also are subclassified as P2X or P2Y receptors. To date, seven mammalian P2X receptors ($P2X_{1-7}R$) that are ligand-gated ion channels and five mammalian P2Y receptors ($P2Y_1R$, $P2Y_2R$, $P2Y_4R$, $P2Y_6R$, and $P2Y_{11}R$) have been cloned. P2Y receptors are GPCRs that are mainly coupled to phospholipase C via G_q proteins. Although the individual pharmacological and biochemical profile of cloned P1 and P2 receptor subtypes have been defined, the assignment of each receptor type to the various purinergic functions in tissues or cells has been limited by the low selectivity and cross-reactivity of available purinergic ligands. The diverse aspects of purinergic functions also may predict a greater number of purinergic receptor subtypes than expected from cloning studies (2–9). In addition, these receptor-mediated events can be modulated either by cross-talk with other receptor systems (10, 11).

Recently, a significant amount of GPCR has been reported to exist in a homomeric (12–17) and heteromeric assembly (18–25). Although most heteromeric assemblies consist of different subtypes of the same receptor family, several combinations such as somatostatin receptor/D_2R and β_2-adrenergic receptor/opioid receptor (26, 27) have been reported to form heterodimers between truly different GPCRs (with only ≈30% sequence homology). We therefore predicted that, like other GPCRs, P1 receptors can potentially form heteromeric complexes with distinct types of GPCRs through direct association. In fact, previous radioligand binding and biochemical studies (24, 25, 28–30) indicated that A_1R could be arranged in dimeric complexes with related proteins or GPCRs. However, to date, no evidence of direct interaction between G protein-coupled P1 and P2 receptors that induces functional changes in cells or tissues has been obtained, although functional interactions between A_1R and P2YR has been previously described (31). A recent study showed that $P2Y_1R$ localized in neuronal cells of the hippocampus, midbrain, and subthalamic nucleus and associated regions (32) and that A_1R localized in the cerebral cortex, hippocampus, and thalamus, especially in the neuronal cells of these regions (33). Therefore, a significant portion of A_1R and $P2Y_1R$ distributed in the central nervous system is likely to colocalize in the overlap regions and thereby exert new functions. The purpose of this study is to determine whether P1 and P2 receptors, in this case A_1R and $P2Y_1R$, can form a heterooligomer that exerts novel pharmacological and functional characteristics with a potential role in the purinergic-signaling cascade.

PHARMACOLOGY

Materials and Methods

cDNA Construction and Cell Transfection. The incorporation of sequences encoding the hemagglutinin (HA) epitope tag (YPYDVPDYA) and the Myc epitope tag (EQKLISEEDL) into rat A_1R and rat $P2Y_1R$ or $P2Y_2R$ genes, respectively, was performed by PCR. Each epitope was positioned immediately before the first methionine of the appropriate gene. Purified full-length cDNA of HA-A_1R was subcloned into pcDNA3 and purified full-length cDNAs of Myc-$P2Y_1R$ and Myc-$P2Y_2R$ were subcloned into pcDNA3.1. cDNAs encoding rat $P2Y_1R$ and $P2Y_2R$ were gifts of G. I. Bell (University of Chicago, Chicago,

This paper was submitted directly (Track II) to the PNAS office.

Abbreviations: GPCR, G protein-coupled receptor; A_1R, A_1 adenosine receptor; $P2Y_1R$, $P2Y_1$ receptor; $P2Y_2R$, $P2Y_2$ receptor; D_2R, dopamine D_2 receptor; HA, hemagglutinin; PTX, pertussis toxin; NECA, 5′-*N*-ethylcarboxamidoadenosine; DPCPX, 8-cyclopentyl-1,3-dipropylxanthine; CPA, N^6-cyclopentyladenosine; ADPβS, adenosine 5′-*O*-(2-thiotriphosphate); MRS2179, N^6-methyl-2′-deoxyadenosine-3′,5′-bisphosphate; FSK, forskolin; IP_3, inositol 1,4,5-trisphosphate.

‡To whom reprint requests should be addressed at: Department of Molecular and Cellular Neurobiology, Tokyo Metropolitan Institute for Neuroscience, 2-6 Musashidai, Fuchu, Tokyo 183-8526, Japan. E-mail: nakata@tmin.ac.jp.

The publication costs of this article were defrayed in part by page charge payment. This article must therefore be hereby marked "*advertisement*" in accordance with 18 U.S.C. §1734 solely to indicate this fact.

IL) and W. R. Rice (Children's Hospital Medical Center, Cincinnati, OH), respectively. Myc-dopamine D_2 receptor (D_2R) cDNA was kindly donated by T. Haga (Tokyo University, Tokyo). The generation of each construct was confirmed by sequencing analysis. DNA (2 μg) was mixed with Effectene transfection reagent (Qiagen, Chatsworth, CA), and the mixture was diluted with DMEM and added to 30–50% confluent HEK293T cells plated on 100-mm dishes. The transfected HEK293T cells were cultured in DMEM with 10% FBS. Cell membranes for immunoprecipitation and Western blotting were prepared from the cells 48 h after the transfection. For adenylyl cyclase and inositol 1,4,5-trisphosphate (IP_3) assays, the cells were passaged to 24-well and 12-well plates, respectively, 48 h after the transfection and cultured for another 24 h at 37°C. When indicated, cells were pretreated with pertussis toxin (PTX) for 16–20 h at a concentration of 100 ng/ml.

Membrane Preparation, Coimmunoprecipitation, and Western Blotting. For HEK293T cell membrane preparation, cells expressing single or combinations of receptors ($\approx 2 \times 10^7$ cells) were washed twice with PBS and collected with a rubber policeman in hypotonic lysis buffer containing 50 mM Tris-acetate buffer, pH 7.4, with a protease-inhibitor mixture (Roche Diagnostics). Cells were disrupted by sonication and subjected to low-speed centrifugation to remove organelles and nuclei. The resulting supernatant was subjected to centrifugation at 30,000 $\times$ *g* for 20 min, and precipitated cell membranes were collected, washed twice, resuspended in the lysis buffer, and stored at −80°C. The membranes were solubilized by incubation with Tx buffer (50 mM Tris·HCl buffer, pH 7.4, containing 1% Triton X-100, 300 mM NaCl, 100 mM iodoacetamide, and a protease-inhibitor mixture) for 60 min at 4°C on a rotator. The mixture was centrifuged at 18,500 $\times$ *g* for 20 min, and the supernatant was collected as the cell membrane lysate. In some instances, the extracted cell membrane lysate was treated with 0.7 units *N*-glycosidase F for 3 h at 37°C. An aliquot of the cell membrane lysate (500 μg protein) was precleared with 30 μl of Protein G-agarose (50% suspension in PBS) at 4°C for 30 min on a rotator. The Protein G-agarose was then removed by centrifuging the lysate at 18,500 $\times$ *g* for 5 min at 4°C. Subsequently, the precleared cell membrane lysate was incubated with 1 μg of anti-Myc 9E10 mAb (Roche Diagnostics) or anti-HA 3F10 mAb (Roche Diagnostics) for 60 min at 4°C on a rotator, and then 50 μl of Protein G-agarose was added to the mixture. The incubation was continued for an additional 120 min at 4°C. The immune-complex was washed three times with Tx buffer, and subsequently it was eluted from Protein G-agarose by the addition of 50 μl of the sample buffer used for SDS/PAGE. An appropriate amount of immunoprecipitated proteins was subjected to SDS/PAGE, after which the protein on the gel was electrotransferred to a nitrocellulose membrane. After blocking with 5% skim milk dissolved in washing buffer (0.1% Tween 20 in Tris·HCl-buffered saline), HA-A_1R, Myc-$P2Y_1R$, Myc-$P2Y_2R$, or Myc-D_2R on the blot were detected by using anti-HA 3F10 mAb (50 ng/ml) or anti-Myc PL14 mAb (1 μg/ml, Medical and Biological Laboratories), followed by horseradish peroxidase-conjugated goat anti-rat IgG antibody (for anti-HA mAb) or goat anti-mouse IgG antibody (for anti-Myc mAb). The reactive bands were visualized with enhanced chemiluminescent substrates (Pierce).

Receptor Binding and Functional Assays. For the assay of A_1R antagonist binding, 10 μg of cell membranes was incubated with 2 nM [^{3}H]8-cyclopentyl-1, 3-dipropylxanthine (DPCPX) (87.0 Ci/mmol, New England Nuclear) containing 2 units/ml adenosine deaminase (Sigma), 5 mM $MgCl_2$, and 50 mM Tris-acetate buffer (pH 7.4) for 60 min at 25°C in the absence or presence of various concentrations of unlabeled ligands. For agonist binding, 30–50 μg of membrane proteins was incubated with 40 nM [^{3}H]5′-*N*-ethylcarboxamidoadenosine (NECA) (27.0 Ci/mmol, Amersham Pharmacia) under the same conditions described above. Saturation and competition binding assays were performed as described (3). In some cases, nonspecific binding of [^{3}H]NECA was determined in the presence of cold NECA (10 μM). Values for the estimated concentration for dissociation constant (K_i) were determined from displacement curves by using GRAPHPAD PRISM 2.0 (GraphPad, San Diego).

cAMP production was measured by a cAMP EIA system (Amersham Pharmacia). Briefly, transfected HEK293T cells (1×10^5 cells/well) in serum-free DMEM were preincubated with 50 μM Ro 20–1724 for 10 min and then stimulated with the indicated concentrations of agonists for 10 min in the presence of 10 μM forskolin (FSK). The reactions were terminated by adding HCl (0.1 M final concentration). cAMP extracted from cells was quantified as described in the manufacturer's manual. The production of IP_3 was determined by using an IP_3 assay kit (Amersham Pharmacia). The transfected cells (3×10^5 cells/well) were preincubated for 30 min at 37°C with serum-free DMEM containing 20 mM LiCl (to inhibit inositol 1-phosphatase) in the presence or absence of antagonists. The cells then were incubated with either N^6-cyclopentyladenosine (CPA) or adenosine 5′-*O*-(2-thiotriphosphate) (ADPβS) at various concentrations in 500 μl of Na-Hepes-buffered saline [140 mM NaCl, 4.7 mM KCl, 1.13 mM $MgCl_2$, 10 mM glucose, 1 mM $CaCl_2$, and 10 mM Hepes (pH 7.4)]. The reaction was terminated at various time points by aspiration of the solution followed by the addition of 500 μl of 4% (vol/vol) $HClO_4$ and incubation for 20 min on ice. After the cell suspension was centrifuged, the supernatant was neutralized with 1.5 M KOH in 10 mM Hepes. The supernatant was assayed for IP_3 by a competitive radioreceptor assay according to the manufacturer's instruction.

Immunocytochemistry. For fluorescence immunocytochemistry, 48 h after transfection cells were fixed for 30 min in 4% paraformaldehyde in PBS, permeabilized with 0.25% Triton X-100, and incubated with primary antibody against HA tag or Myc tag for 90 min at room temperature. Rat anti-HA 3F10 mAb was visualized with Cy3-conjugated goat anti-rat IgG antibodies (Jackson ImmunoResearch). Mouse anti-Myc 9E10 mAb was detected by FITC-conjugated goat anti-mouse IgG antibody (Jackson ImmunoResearch). Fluorescent images were obtained with a Zeiss LSM 410 confocal microscope. The extent of overlap of the two signals was determined by the software for the Carl Zeiss LSM 4 Laser Scan Microscope.

Results

Association of A_1R and $P2Y_1R$ in Coexpressed HEK293T Cells. We transiently cotransfected HA-A_1R and Myc-$P2Y_1R$ cDNAs into HEK293T cells and examined whether A_1R and $P2Y_1R$ associate with each other as a heteromeric complex by conducting immunoprecipitation experiments using whole-cell membrane lysates (Fig. 1). The addition of an epitope, HA or Myc, to the NH_2 terminus of these receptors had no effect on the electrophoretic mobility of the receptors visualized on SDS/PAGE (data not shown). Western blots of cell membranes expressing HA-A_1R exhibited anti-HA reactive bands of predicted molecular mass (A_1R, 35 kDa; ref. 34) in addition to a band of lower molecular mass of 31 kDa (Fig. 1*A*). Western blots of cell membranes expressing Myc-$P2Y_1R$ showed anti-Myc reactive bands of 45, 42, and 37 kDa (Fig. 1*A*). The predicted molecular mass of $P2Y_1R$ has been reported as 42 kDa (35). The lower molecular mass bands were likely to be the deglycosylated form of the receptors, because most bands shifted to a position of the low molecular mass band after treatment with *N*-glycosidase F (Fig. 1*A*). We found that anti-Myc antibody precipitated HA-A_1R in addition to Myc-$P2Y_1R$ from cells coexpressing HA-A_1R/Myc-

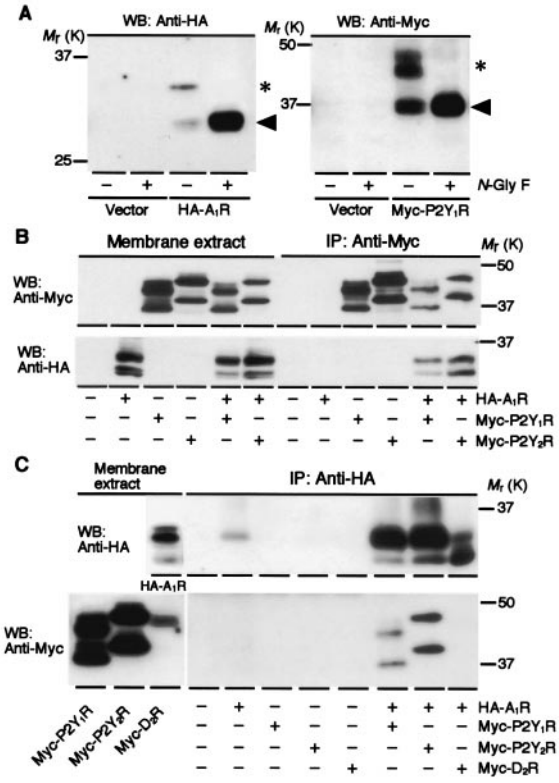

Fig. 1. Association of A_1R and $2Y_1R$ in $A_1R/P2Y_1R$-transfected HEK293T cells. (*A*) Western blot (WB) analysis of cell membranes expressing HA-A_1R (*Left*) and Myc-$P2Y_1R$ (*Right*). Cell lysates that had been treated by *N*-glycosidase F (+) for 3 h at 37°C were subjected to Western blotting. HA-A_1R and Myc-$P2Y_1R$ were detected by anti-HA and anti-Myc antibodies, respectively. The control (−) without treatment by *N*-glycosidase F also was subjected to Western blotting. The apparent molecular masses of the glycosylated (*) and deglycosylated (arrowheads) HA-A_1R are 35 and 31 kDa, respectively. The apparent molecular masses of the glycosylated Myc-$P2Y_1R$ are 45 and 42 kDa (*), and the deglycosylated Myc-$P2Y_1R$ is 37 kDa (arrowheads). (*B*) Coimmunoprecipitation of cell lysates by anti-Myc antibody. Anti-Myc antibody precipitated Myc-$P2Y_1R$ (*Upper,* the 9th and 11th lanes from the left) and Myc-$P2Y_2R$ (*Upper,* lanes 10 and 12 from the left), and coimmunoprecipitated HA-A_1R with Myc-$P2Y_1R$ (*Lower,* lane 11 from the left) or Myc-$P2Y_2R$ (*Lower*, lane 12 from the left). (*C*) Coimmunoprecipitation of cell lysates by anti-HA antibody. In addition to HA-A_1R, anti-HA antibody coimmunoprecipitated Myc-$P2Y_1R$ from the cell membrane lysates coexpressing HA-A_1R/Myc-$P2Y_1R$ (*Lower*, lane 9 from the left). Myc-$P2Y_2R$ also was coimmunoprecipitated by anti-HA antibody along with HA-A_1R from the cell lysates coexpressing HA-A_1R/Myc-$P2Y_2R$ (*Lower*, lane 10 from the left). In contrast, Myc-D_2R was not immunoprecipitated from the cell lysates coexpressing HA-A_1R/Myc-D_2R (*Lower*, lane 11 from the left) by anti-HA antibody. Data are representative of 2–4 independent experiments.

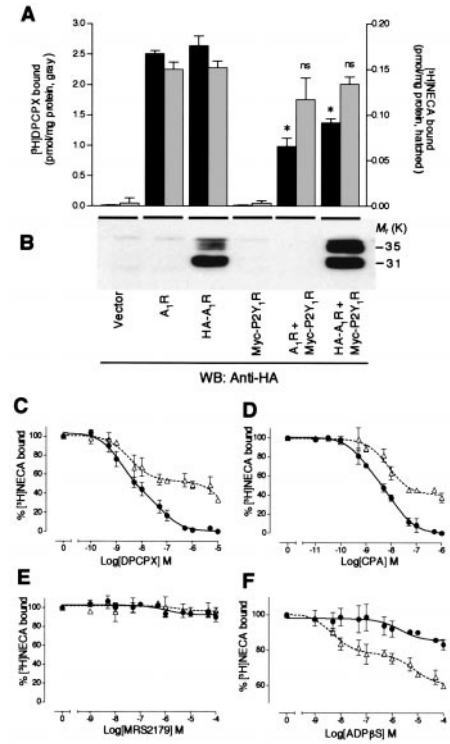

Fig. 2. Coexpression with $P2Y_1R$ modulates A_1R binding pharmacology. (*A*) The [^{3}H]DPCPX (gray columns, left *y axis*) and [^{3}H]NECA (hatched columns, right *y* axis) binding activities of cell membranes expressing A_1R (nontagged and HA-tagged) together with Myc-$P2Y_1R$. The binding affinity of adenosine receptor antagonist [^{3}H]DPCPX was significantly reduced by the coexpression of $A_1R/P2Y_1R$, whereas [^{3}H]NECA binding activity was not significantly affected. Data represent the means ± SEM of the [^{3}H]DPCPX or [^{3}H]NECA-specific bound values. Results from three independent experiments performed in duplicate are shown. * indicate statistically significant difference from respective cells expressing A_1R or HA-A_1R alone ($n = 3$, $P < 0.05$, Student's *t* test). ns, not significant. (*B*) Western blotting (WB) of transfected cell lysates using anti-HA antibody. The blot showed the slightly higher expression of HA-A_1R protein in cotransfected cells (lane 6 from the left) than that in HA-A_1R-transfected cells (lane 3 from the left). Displacement of [^{3}H]NECA (40 nM) binding with transfected cell membranes by DPCPX (*C*), CPA (*D*), MRS2179 (*E*), and ADPβS (*F*). Membranes from HA-A_1R-transfected (*C–F,* ●) or HA-A_1R/$P2Y_1R$-transfected (*C–F*, △) cells were incubated with indicated concentrations of each ligand. The [^{3}H]NECA concentrations were selected to ensure maximal saturation binding. The K_i values for A_1R ligands, CPA and DPCPX, are shifted about 2-fold toward lower potencies, whereas the K_i value for potent $P2Y_1R$ agonist ADPβS is shifted 400-fold toward higher potency in cotransfected cells. The heteromeric complex also reduces the binding efficacy to DPCPX (70% versus 100% at 10 μM) and to CPA (60% versus 100% at 1 μM). Data represent the means ± SEM of the percentage of [^{3}H]NECA-specific bound values. Results from three independent experiments performed in duplicate are shown.

$P2Y_1R$ (Fig. 1*B*). Conversely, anti-HA antibody precipitated both Myc-$P2Y_1R$ and HA-A_1R from cells coexpressing HA-A_1R and Myc-$P2Y_1R$ (Fig. 1*C*). Such counterimmunoprecipitation was not observed with the admixture of cell membranes expressing each receptor individually (data not shown). For comparison, Myc-$P2Y_2R$ or Myc-D_2R instead of Myc-$P2Y_1R$ was cotransfected with HA-A_1R. Anti-HA antibody precipitated Myc-$P2Y_2R$ along with HA-A_1R from Myc-$P2Y_2R$/HA-A_1R coexpressed cells (Fig. 1 *B* and *C*). However, Myc-D_2R was not immunoprecipitated along with HA-A_1R by anti-HA antibody (Fig. 1*C*). It also was confirmed that neither Myc-$P2Y_1R$ nor Myc-$P2Y_2R$ was immunoprecipitated by the anti-HA antibody or vice versa for the HA-A_1R from cell membrane extracts expressing only Myc-$P2Y_1R$ or Myc-P_2Y_2R. These findings indicate that A_1R can form heteromeric complexes with $P2Y_1R$ or $P2Y_2R$ when transfected simultaneously in HEK293T cells.

Coexpression with $P2Y_1R$ Modulates A_1R Binding Pharmacology. We examined the ligand-binding properties of HEK293T cell membranes expressing A_1R and $P2Y_1R$ by using A_1R selective antagonist [^{3}H]DPCPX or nonselective adenosine receptor agonist [^{3}H]NECA. It should be noted that no significant specific binding of these radioligands was observed with cell membranes expressing Myc-$P2Y_1R$ alone or mock plasmid. As shown in Fig. 2*A*, cell membranes expressing HA-A_1R showed [^{3}H]DPCPX and [^{3}H]NECA binding activities similar to those of cell membranes expressing intact A_1R, suggesting that N-terminal modification of A_1R with HA tag did not alter ligand-binding activities. In contrast, cell membranes coexpressing HA-A_1R/Myc-$P2Y_1R$ or A_1R/Myc-$P2Y_1R$ showed significantly lower [^{3}H]DPCPX binding activity than did cell membranes expressing

PHARMACOLOGY

Table 1. Comparison of the ligand-binding properties of A_1R and its heteromers

	Radioligand					
	[^{3}H]DPCPX		[^{3}H]NECA		[^{3}H]*R*-PIA	
	K_D, nM	B_{max}, pmol/mg	K_D, nM	B_{max}, pmol/mg	K_D, nM	B_{max}, pmol/mg
A_1R	1.3 ± 0.14	3.5 ± 0.12	—	—	—	—
HA-A_1R	1.2 ± 0.12	3.6 ± 0.11	3.4 ± 1.2	0.11 ± 0.07	0.85 ± 0.3	0.09 ± 0.02
HA-A_1R + Myc-$P2Y_1R$	1.2 ± 0.1	1.9 ± 0.05*	3.5 ± 1.8	0.09 ± 0.03	3.1 ± 1.7*	0.08 ± 0.03

For an A_1R antagonist [^{3}H]DPCPX saturation experiment, 10 μg of membrane protein was incubated with 0.2–10 nM [^{3}H]DPCPX containing 2 units/ml adenosine deaminase, 5 mM $MgCl_2$, and 50 mM Tris-acetate buffer, pH 7.4 for 60 min at 25°C. Nonspecific binding was measured in the presence of 1 μM XAC. For agonist [^{3}H]NECA and [^{3}H]*R*-PIA saturation experiment, 30–50 μg of membrane proteins was incubated with 2–50 nM radioligands in the same condition described above. The binding of these ligands to Myc-$P2Y_1R$ was not detected. *, $P < 0.05$ (Student's *t* test, n = 3).

HA-A_1R alone ($P < 0.05$, Student's *t* test), despite the fact that the expression level of HA-A_1R protein in cotransfected cell membranes was equal or even higher than that of cell membranes transfected with HA-A_1R alone, as judged by Western blotting (Fig. 2*B*). The decrease in [^{3}H]DPCPX binding activity observed with the HA-A_1R/Myc-$P2Y_1R$-transfected cell membranes was mainly due to the decrease in B_{max} values from saturation binding assays (Table 1). In contrast, no significant differences in [^{3}H]NECA binding were observed between HA-A_1R-transfected and HA-A_1R/Myc-$P2Y_1R$-transfected cell membranes, as shown in Fig. 2*A* and Table 1. Furthermore, a significant reduction of a selective A_1R agonist, [^{3}H]R-N^6-phenylisopropyladenosine (*R*-PIA), binding with HA-A_1R/Myc-$P2Y_1R$-transfected cell membranes also was observed. The decrease in [^{3}H]*R*-PIA binding was mainly due to the increase in K_D values, as determined from saturation binding assays (Table 1). Because these changes in ligand-binding pharmacology were not observed with the admixture of cell membranes expressing each receptor individually (data not shown), the expression of this novel binding activity might require *in situ* direct association of A_1R with $P2Y_1R$ and it may not result from nonspecific aggregation between these receptors. The difference in the B_{max} values between antagonist and agonist interactions is likely due to the uncoupling of A_1R and G protein in the transfected cells, which is often reported in other receptor systems. We further examined ligand-binding pharmacology of the cotransfected cell membranes using [^{3}H]NECA by competition experiments with other purinergic ligands (Fig. 2 *C–F*). The apparent binding potency and efficacy of both A_1R-selective antagonist DPCPX (Fig. 2*C*) and A_1R-selective agonist CPA (Fig. 2*D*) to the [^{3}H]NECA binding site were reduced in the cotransfected cells. Selective $P2Y_1R$ antagonist N^6-methyl-2′-deoxyadenosine-3′,5′-bisphosphate (MRS2179) failed to displace [^{3}H]NECA bound to HA-A_1R-transfected and HA-A_1R/Myc-$P2Y_1R$-transfected cell membranes (Fig. 2*E*). A potent $P2Y_1R$ agonist, ADPβS, was found to be quite active in displacing the ligands from the [^{3}H]NECA binding site of cotransfected cell membranes with K_i values of 0.38 ± 0.05 nM (high-affinity site) and 610 ± 85 nM (low-affinity site) (Fig. 2*F*, △). In contrast, ADPβS at the 10^{-6} M range slightly inhibited [^{3}H]NECA binding of cell membranes expressing HA-A_1R alone (K_i = 1,670 ± 98 nM, Fig. 2*F*, ●). Breakdown products of ADPβS that might have been produced during the incubation may explain the modest inhibitory effect of ADPβS on [^{3}H]NECA binding with cell membranes expressing HA-A_1R.

Adenylyl Cyclase Coupling in Cotransfected Cells. Next we attempted to determine whether heteromerization leads to alterations in cellular functional coupling. To that end, we studied A_1R agonist-induced adenylyl cyclase inhibition, a main index of A_1R function, in cotransfected cells (Fig. 3). The cells expressing A_1R alone revealed an inhibition of FSK-stimulated cAMP accumulation by CPA in a dose-dependent manner, with the estimated concentration for half-maximal response (IC_{50}) of 0.42 ± 0.1 nM to a maximum inhibition of 70 ± 6%. This activity was completely abolished by pretreatment of the cells with PTX (Fig. 3*A*). CPA-induced inhibition of FSK-stimulated adenylyl cyclase activity also was detected with the estimated IC_{50} value of 1.0 ± 0.12 nM in the cells coexpressing A_1R/$P2Y_1R$. This activity also was abolished by PTX treatment (Fig. 3*A*). The potency of adenylyl cyclase attenuation by CPA was reduced significantly in the coexpressing cells compared with cells expressing A_1R alone ($P < 0.05$, Student's *t* test). The treatment of cells expressing A_1R alone with ADPβS revealed no changes in FSK-stimulated cAMP production (Fig. 3*B*). Activation of $P2Y_1R$-transfected cells with ADPβS did not lead to a significant change in FSK-evoked cAMP levels (data not shown). In cells coexpressed with A_1R and $P2Y_1R$, ADPβS markedly reduced

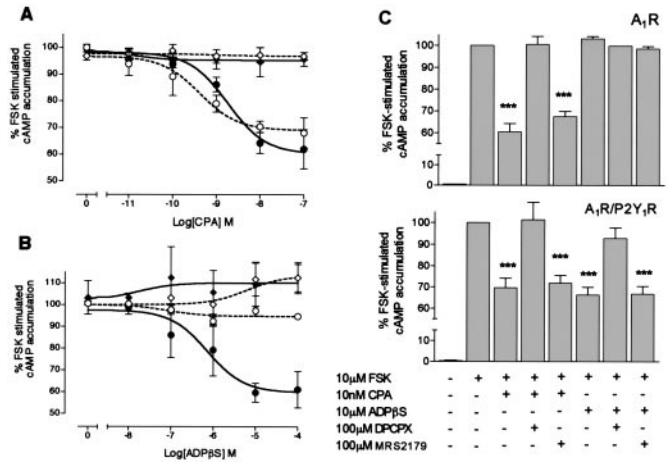

Fig. 3. Generation of $P2Y_1R$ agonist-sensitive adenylyl cyclase inhibition of A_1R. (*A* and *B*) Concentration-dependent reduction of maximal FSK (10 μM)-stimulated intracellular cAMP accumulation by CPA (*A*) or ADPβS (*B*) in A_1R/$P2Y_1R$-transfected cells. The attenuation was blocked by the PTX pretreatment (100 ng/ml, 16 h). Dotted line, cells expressing HA-A_1R alone; solid line, cells coexpressing HA-A_1R and Myc-$P2Y_1R$; circles, nontreated cells; diamonds, PTX-pretreated cells. The 100% values of cAMP for the cells transfected with HA-A_1R and HA-A_1R plus Myc-$P2Y_1R$ were 72 ± 14 and 67 ± 19 pmol/10^5 cells, respectively (mean ± SEM, n = 5). Estimated IC_{50} values are shown in the text. (*C*) Pretreatment of cells with A_1R antagonist DPCPX, but not $P2Y_1R$ antagonist MRS2179, significantly inhibited maximal ADPβS-induced adenylyl cyclase attenuation in the A_1R/$P2Y_1R$-transfected cells. (*Upper*) HA-A_1R transfected cells. (*Lower*) HA-A_1R/Myc-$P2Y_1R$ cotransfected cells. The 100% values of cAMP for the cells transfected with HA-A_1R and HA-A_1R/Myc-$P2Y_1R$ were 70 ± 12 and 71 ± 17 pmol/10^5 cells, respectively (mean ± SEM, n = 5). Data represent the means ± SEM of the percentage of FSK-induced cAMP accumulation values. Results from 3–5 independent experiments performed in duplicate are shown. ***, $P < 0.01$, Student's *t* test.

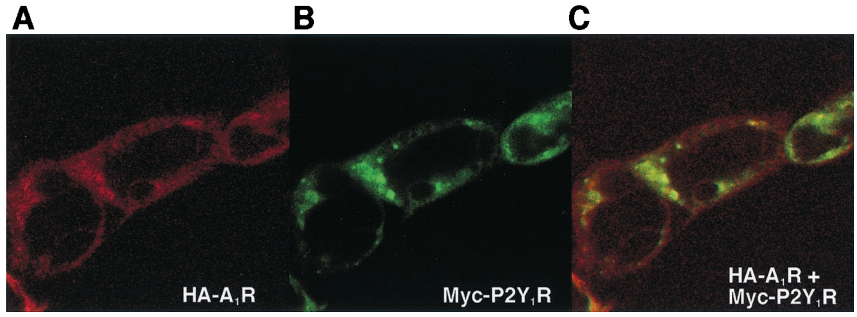

Fig. 4. Confocal imaging of HEK293T cells expressing HA-A_1R/Myc-$P2Y_1$R. HA-A_1R (*A*, Cy3, red) and Myc-$P2Y_1$R (*B*, FITC, green) were detected by using double fluorescent immunohistochemistry. (*C*) The product of merging *A* and *B*, showing the colocalization of HA-A_1R and Myc-$P2Y_1$R in cotransfected HEK293T cells (yellow).

FSK-evoked adenylyl cyclase activity in a concentration-dependent manner, with the estimated IC_{50} value of 730 ± 35 nM, to a maximum inhibition of 62 ± 9%. PTX treatment resulted in complete loss of the dose-dependent activity of ADPβS, suggesting the involvement of a PTX-sensitive $G_{i/o}$ protein (Fig. 3*B*). We next examined whether the ADPβS-induced adenylyl cyclase inhibition in coexpressed cells was mediated through the ligand-binding site of A_1R (Fig. 3*C*). In both A_1R-expressing cells and A_1R/$P2Y_1$R-coexpressing cells, CPA (10 nM) maximally inhibited the FSK-evoked adenylyl cyclase activity to virtually identical extents. This inhibitory effect was blocked in the presence of A_1R antagonist DPCPX. When cells coexpressing A_1R/$P2Y_1$R were pretreated with DPCPX, however, the ADPβS-evoked adenylyl cyclase inhibition was decreased by ≈95%, whereas MRS2179 had no effect on the ADPβS-evoked adenylyl cyclase inhibition. Taken together, these results suggest that ADPβS exerts the adenylyl cyclase inhibitory activity through xanthine-sensitive ligand-binding sites of A_1R via $G_{i/o}$ protein-linked effector system.

IP_3 Production in Cotransfected Cells. To analyze the effect of A_1R/$P2Y_1$R heteromeric formation on the $P2Y_1$R-effector systems, we examined the production of intracellular IP_3 stimulated by $P2Y_1$R agonist ADPβS in cotransfected cells. ADPβS at its maximum effective dose of 10 μM induced a 3.1 ± 0.5-fold (n = 3, duplicates in each experiment) increase in IP_3 production over basal levels in cells expressing A_1R/$P2Y_1$R. The time course of the ADPβS-induced IP_3 production was similar to that of the cells expressing $P2Y_1$R alone. Both responses peaked at 15 s after the addition of ADPβS and declined rapidly toward basal levels in 2 min. The dose-dependent potency of ADPβS (EC_{50} = 3.5 ± 0.6 μM), however, slightly decreased in cotransfected cells ($P < 0.05$, Student's t test, $n = 3$) compared with the potency of ADPβS in $P2Y_1$R-transfected cells (EC_{50} = 1.4 ± 0.4 μM), whereas there were no significant differences in the maximum responses induced by ADPβS between cells expressing $P2Y_1$R and cells expressing A_1R/$P2Y_1$R. We confirmed that the amount of $P2Y_1$R as determined by Western blotting did not change upon coexpression with A_1R. ADPβS (10 μM) did not stimulate IP_3 production in A_1R-transfected cells, and CPA (10 nM) did not stimulate $P2Y_1$R- and A_1R/$P2Y_1$R-transfected cells. Also, the simultaneous addition of CPA (10 nM) and ADPβS (10 μM) in the cotransfected cells did not stimulate IP_3 production any more than did the stimulation by ADPβS alone.

Double-Immunostaining of A_1R/$P2Y_1$R in Cotransfected Cells. We studied the subcellular distribution of HA-A_1R and Myc-$P2Y_1$R in cotransfected cells by confocal laser microscopy (Fig. 4). When expressed in HEK293T cells individually, HA-A_1R and Myc-$P2Y_1$R were localized in the vicinity of the plasma membranes (data not shown). Images taken at the microscopic level with a ×63 objective of cotransfected cells that were double labeled for HA-A_1R (red) and Myc-$P2Y_1$R (green) are shown (Fig. 4 *A* and *B*). Both receptors were expressed prominently near the plasma membranes. When the images are merged by using the confocal assistant software, there is a striking overlap (intense yellow spots) in the distribution of the two receptors (Fig. 4*C*). The extent of overlap pixels of the two signals was 35.4 ± 9.6% (n = 3). The immunostaining of unpermealized cells also was performed with similar results (data not shown). The fact that this colocalization occurred over plasma membranes supports the heteromeric association of A_1R and $P2Y_1$R.

Discussion

The present study provides biochemical, pharmacological, and functional evidence for the existence of a heteromeric complex between P1 and P2 receptors. We also report on heteromer formation between distinct G protein-coupled purinergic receptors with very low amino acid sequence homology (less than 5% amino acid sequence homology between A_1R and $P2Y_1$R), although there is increasing biochemical and functional evidence for oligomerization of GPCRs (36, 37).

Immunoprecipitation (Fig. 1) and double immunostaining (Fig. 4) experiments showed the existence of A_1R/$P2Y_1$R heteromer in HEK293T cells when cotransfected with A_1R and $P2Y_1$R. Ligand binding (Fig. 2, Table 1) and functional experiments (Fig. 3) indicate that the A_1R/$P2Y_1$R heteromeric complex altered the pharmacology of these receptors, i.e., the A_1R was altered to have $P2Y_1$R-like agonistic pharmacology. The structural requirements for the A_1R/$P2Y_1$R heteromeric association are not known, although several other studies reported that the C tails of γ-aminobutyric acid type B receptor (21), the extracellular amino-terminal domain for the bradykinin B_2 receptors (17), and the intracellular third loop for the β-adrenergic receptors (12) may represent monomeric or oligomeric interfaces. In the case of A_1R/$P2Y_1$R heteromer, the C tail deletion mutant of A_1R was still able to associate with $P2Y_1$R and also with $P2Y_2$R in HEK293T cells (unpublished results), which suggests that the C tail of A_1R is not required for the heteromeric association with $P2Y_1$R or $P2Y_2$R. The precise structural requirements for the association of A_1R with $P2Y_1$R remain to be elucidated. It also remains to be further investigated whether direct receptor association between P1 and P2 receptor is restricted to the A_1R and $P2Y_1$R subtypes. We found that the complex between A_1R and $P2Y_2$R can be formed, although the pharmacology or cellular effector systems of A_1R/$P2Y_2$R heteromeric complex have not been studied. This finding suggests that hetero-oligomerization between subclasses of purinergic receptors may be a widespread phenomenon.

In this study, we observed significant changes in the ligand-binding properties in the heteromers. Ligand-binding studies revealed a significant reduction of A_1R-agonist and A_1R-

antagonist binding in the cotransfected cell membranes. In contrast, we observed a significant 400-fold increase in the binding affinity of ADPβS, a potent $P2Y_1R$ agonist, for the $A_1R/P2Y_1R$-transfected cell membranes. It is likely that a physical association of A_1R with $P2Y_1R$ induced ligand-binding sites with A_1R-$P2Y_1R$ hybrid selectivity. In other words, the modified ligand-binding pocket of A_1R in the heteromer now appears to fit well to a $P2Y_1R$ agonist but slightly less well to A_1R ligands.

It should be interesting to examine functional changes in the cotransfected cells, because A_1R is a GPCR coupled to adenylyl cyclase via $G_{i/o}$ proteins, whereas $P2Y_1R$ is a GPCR coupled to phospholipase C via G_q proteins. The heteromerization resulted in a significant modification of cellular functions (cAMP, IP_3), as shown in Fig. 3. We showed that a potent $P2Y_1R$ agonist ADPβS was able to couple with a PTX-sensitive adenylyl cyclase system only when A_1R and $P2Y_1R$ were coexpressed in HEK293T cells. Because an ADPβS-evoked response in adenylyl cyclase activity was blocked by either A_1R antagonist or PTX but was not blocked by $P2Y_1R$ antagonist, ADPβS is likely to exert its activity via the A_1R ligand-binding site. In contrast, no major alterations in ADPβS-evoked phospholipase C activity (IP_3 production) was induced by the heteromer formation, although we did observe a slight decrease in the affinity of $P2Y_1R$ to the cotransfected cells. These results indicate again that the heteromeric formation between A_1R and $P2Y_1R$ produces functional changes that are preferential to adenylyl cyclase coupling.

Although several studies indicate the presence of atypical subtypes of P2YRs (4–9) that are sensitive to P1 receptor antagonist theophylline or PTX, a molecular basis for these observations has not been well described. A P2Y-like receptor coupled to the $G_{i/o}$ family of G proteins has been observed in rat glioma C6 cells, which can be selectively activated by AMP derivatives, although its identity is unclear (9). Mendoza-Fernandez *et al.* (4) demonstrated that ATP inhibited the synaptic release of glutamate by direct activation of P2Y receptors that are PTX- and 8-cyclopentyltheophylline (P1 receptor antagonist)-sensitive, and suramin-, pyridoxalphosphate-6-azophenyl-2′,4′-disulfonic acid-, and reactive blue 2 (P2 receptor antagonists)-insensitive. They proposed to classify them as theophylline-sensitive P2Y receptors (4). Thus, heteromerization between purinergic receptors that produce a hybrid pharmacology as shown in this study may help to explain undefined physiological functions of purines in various tissues and cells.

In conclusion, this work shows that signal modification is triggered by receptor heteromerization of P1 and P2 purinergic receptors. Heteromerization of G protein-coupled purinergic receptors may be a mechanism for the control of purinergic functions, although it remains to be established whether such heteromerization occurs in a living organism, because artifacts may arise from the aggregation of GPCRs in overexpression experiments.

We are grateful to Dr. G. I. Bell for providing rat $P2Y_1R$ cDNAs and Dr. W. R. Rice for rat $P2Y_2R$ cDNA. We thank Dr. T. Haga and R. Takahashi for donating Myc-tagged dopamine D_2 receptor cDNA and HEK293T cells, respectively. We also thank Dr. K. Nishi for his help with the confocal microscopy experiments. This work was supported in part by grants for Scientific Research from the Ministry of Education, Science, Sports and Culture of Japan (to O.S. and H.N.), by the Kato Memorial Bioscience Foundation (to O.S.) and also by a Research Grant from the Yamanouchi Foundation for Research on Metabolic Disorders (to H.N.).

1. Ralevic, V. & Burnstock, G. (1998) *Pharmacol. Rev.* **50,** 413–492.
2. Shinozuka, K., Bjur, R. A. & Westfall, D. P. (1988) *Naunyn-Schmiedeberg's Arch. Pharmacol.* **338,** 221–227.
3. Saitoh, Y. & Nakata, H. (1996) *Biochem. Biophys. Res. Commun.* **219,** 469–474.
4. Mendoza-Fernandez, V., Andrew, R. D. & Barajas-López, C. (2000) *J. Pharmcol. Exp. Ther.* **293,** 172–179.
5. Song, S. L. & Chueh, S. H. (1996) *Brain Res.* **734,** 243–251.
6. Ikeuchi, Y., Nishizaki, T., Mori, M. & Okada, Y. (1996) *Eur. J. Pharmacol.* **304,** 191–199.
7. Barajas-López, C., Muller, M. J., Prieto-Gómez, B. & Espinosa-Luna, R. (1995) *J. Pharmcol. Exp. Ther.* **274,** 1238–1245.
8. Koizumi, S. & Inoue, K. (1997) *Br. J. Pharmacol.* **122,** 51–58.
9. Boyer, J. L., Lazarowski, E. R., Chen, X. H. & Harden, T. K. (1993) *J. Pharmcol. Exp. Ther.* **267,** 1140–1146.
10. Quitterer, U. & Lohse, M. J. (1999) *Proc. Natl. Acad. Sci. USA* **96,** 10626–10631.
11. Gao, Z., Chen, T., Weber, M. J. & Linden, J. (1999) *J. Biol. Chem.* **274,** 5972–5980.
12. Hebért, T. E., Moffett, S., Morello, J. P., Loisel T. P., Bichet, D. G., Barret, C. & Bouvier, M. (1996) *J. Biol. Chem.* **271,** 16384–16392.
13. Nimchinsky, E. A., Hof, P. R., Janssen, W. G. M., Morrison, J. H. & Schmauss, C. (1997) *J. Biol. Chem.* **272,** 29229–29237.
14. Bai, M., Trivedi S. & Brown, E. M. (1998) *J. Biol. Chem.* **273,** 23605–23610.
15. George, S. R., Lee, S. P., Varghese, G., Zeman, P. R., Seeman, P., Ng, G. Y. K. & O'Dowd, B. F. (1998) *J. Biol. Chem.* **273,** 30244–30248.
16. Zeng, F. Y. & Wess, J. (1999) *J. Biol. Chem.* **274,** 19487–19497.
17. AbdAlla, S., Zaki, E., Lother, H. & Quitterer, U. (1999) *J. Biol. Chem.* **274,** 26079–26084.
18. Jones, K. A. Borowsky, B., Tamm, J. A., Craig, D. A., Durkin, M. M., Dai, M., Yao, W. J., Johnson, M., Gunwaldsen, C., Huang, L. Y., *et al.* (1998) *Nature (London)* **396,** 674–679.
19. White, J. H., Wise, A., Main, M. J., Green, A., Fraser, N. J., Disney, G. H., Barnes, A. A., Emson, P., Foord, S. M. & Marshall, F. H. (1998) *Nature (London)* **396,** 679–682.
20. Jordan, B. A. & Devi, L. A. (1999) *Nature (London)* **399,** 697–700.
21. Kuner, R., Köhr, G., Grünewald, S., Eisenhardt, G., Bach, A. & Kornau, H-.C. (1999) *Science* **283,** 74–77.
22. Rocheville, M., Lange, D. C., Kumar, U., Sasi, R., Patel, R. C. & Patel, Y. C. (2000) *J. Biol. Chem.* **275,** 7862–7869.
23. AbdAlla, S., Lother, H. & Quitterer, U. (2000) *Nature (London)* **407,** 94–98.
24. Ferré, S., Torvinen, M., Antoniou, K., Irenius, E., Civelli, O., Arenas, E., Fredholm, B. B. & Fuxe, K. (1998) *J. Biol. Chem.* **273,** 4718–4724.
25. Ginés, S., Hillion, J., Torvinen, M., Crom, S. L., Casadó, V., Canela, E. I., Rondin, S., Lew, J. Y., Watson, S., Zoli, M., *et al.* (2000) *Proc. Natl. Acad. Sci. USA* **97,** 8606–8611. (First Published July 11, 2000, 10.1073/pnas.150241097)
26. Rocheville, M., Lange, D. C., Kumar, U., Patel, S. C., Patel, R. C. & Patel, Y. C. (2000) *Science* **288,** 154–157.
27. Jordan, B. A. Trapaidze, N., Gomes, I., Nivarthi, R. & Devi, L. A. (2001) *Proc. Natl. Acad. Sci. USA* **98,** 343–348. (First Published December 26, 2000, 10.1073/pnas.011384898)
28. Frame, L. T., Yeung, S.-M. H., Venter, J. C. & Cooper, D. M. F. (1986) *Biochem. J.* **235,** 621–624.
29. Ciruela, F., Casadó, V., Mallol, J., Canela, E. I., Lluis, C. & Franco, R. (1995) *J. Neurosci. Res.* **42,** 818–828.
30. Ciruela, F., Saura, C., Canela, E. I., Mallol, J., Lluis, C. & Franco, R. (1996) *FEBS Lett.* **380,** 219–223.
31. Gerwins, P. & Fredholm, B. B. (1992) *J. Biol. Chem.* **267,** 16081–16087.
32. Moore, D., Chambers, J., Waldvogel, H., Faull, R. & Emson, P. (2000) *J. Comp. Neurol.* **421,** 374–384.
33. Ochiishi, T., Chen, L., Yukawa, A., Saitoh, Y., Sekino, Y., Arai, T., Nakata, H. & Miyamoto, H. (1999) *J. Comp. Neurol.* **411,** 301–316.
34. Nakata, H. (1993) *Biochim. Biophys. Acta* **1177,** 93–98.
35. Hoffmann, C., More, S., Nicholas, R. A., Harden, T. K. & Jacobson, K. A. (1999) *J. Biol. Chem.* **274,** 14639–14647.
36. Hebért, T. E. & Bouvier, M. (1998) *Biochem. Cell Biol.* **76,** 1–11.
37. Salahpour, A., Angers, S. & Bouvier, M. (2000) *Trends Endocrinol. Metab.* **11,** 163–168.